

PAPER • OPEN ACCESS

The microstructure and electrical resistivity of near-stoichiometric SiC fiber

To cite this article: Weicheng Bai and Ke Jian 2019 *IOP Conf. Ser.: Mater. Sci. Eng.* **490** 022057

View the [article online](#) for updates and enhancements.

The microstructure and electrical resistivity of near-stoichiometric SiC fiber

Weicheng Bai¹, Ke Jian^{1,*}

¹Science and Technology on Advanced Ceramic Fibers and Composites Laboratory, National University of Defense Technology, Changsha 410073, China;

*Corresponding author e-mail: jianke_nudt@163.com

Abstract: SiC fibers with electrical resistivity of different orders of magnitude are of great interest for the fabrication of advanced composites with electromagnetic wave absorbent performance as both structural and functional materials. KD-S and KD-SA fiber produced by National University of Defense Technology were oxidized at 800°C air to get KD-OS and KD-OSA respectively. The microstructure and electrical resistivity of near-stoichiometric SiC fibers (KD-S, KD-OS, KD-SA, KD-OSA) were analyzed and evaluated in detail. The SiC fibers consisted of β -SiC nanocrystallines and free carbon. Apart from KD-OSA, these SiC fibers exhibited a uniquely specific skin-core structure with thin carbon-rich layer of about 25 nm on their surfaces. So the electrical resistivity of KD-OSA was 2961.7 Ω ·cm which was much higher than the rest of the fibers. After testing the porosity and pore size distribution of the fibers, we discover that the pore structure of KD-SA is more abundant than that of KD-S and KD-OS to the extent that the resistivity of KD-SA is higher than that of KD-S and KD-OS.

1. Introduction

Since they were developed by Yajima and coworkers using the precursor derived method^[1-5], SiC fibers with micron scale diameter have attracted increasing attention due to their outstanding properties including high tensile strength, low density, excellent thermal and oxidation resistance, etc.

Among them, resistivity is an important property of SiC fibers. SiC fibers with different electrical resistivity have different uses. For example, the resistivity of NL-400 type SiC fiber is 10⁶~10⁷ Ω ·cm, which is mainly used for radome and aircraft wave transparent material. The NL-500 type SiC fiber has a resistivity of 0.5~5 Ω ·cm, which is mainly used as microwave absorbing material^[13].

At present, Wang Deyin and Hu Tianjiao^[6-9] takes the KD-I which was produced from National University of Defense Technology as the research object. However, there is little research on the

Fund project: NSFC(51403233)

Corresponding author: Ke Jian, Ph.D. Associate Professor, Science and Technology on Advanced Ceramic Fibers and Composites Laboratory, National University of Defense Technology, Changsha 410073, P. R. China, Tel: 0731-84573167, E-mail: jianke_nudt@sina.com



Content from this work may be used under the terms of the [Creative Commons Attribution 3.0 licence](https://creativecommons.org/licenses/by/3.0/). Any further distribution of this work must maintain attribution to the author(s) and the title of the work, journal citation and DOI.

resistivity of third generation fiber. So, this paper is to investigate the factors that affect the resistivity of the third generation fibers.

2. Experimental procedures

2.1 Preparation of SiC fibers

The KD-S fiber was obtained by pyrolysis of EB-cured PCS fibers at 1000°C under hydrogen rich atmosphere of which tensile strength is more than 3.0Gpa. KD-SA fiber and Tyranno-SA use the similar preparation route. It's precursor PACS was prepared from low molecular Polycarbosilane and aluminum acetylacetonate or aluminum chloride^[10,11]. KD-OS and KD-OSA were obtained by oxidizing KD-S and KD-SA at 800°C respectively.

2.2 Characterization

The tensile strength and elastic modulus of the fibers were measured by the single-filament method with a gauge length of 25mm using an Instron-type test machine (Testometric, M350-5CT). The average tensile strength was obtained from the measured results of filaments. The electrical resistivity was calculated from the equation $\rho = \pi R d^2 / 4L$. The resistance of the fiber R was measured using a two-probe direct-current were attached with silver paste to the electrode plates which were 25 mm apart in distance. The fiber diameter d was determined by a spiral micrometer and ρ was the average electrical resistivity of 24 filaments. The morphologies of fibers were observed by utilizing scanning electron microscopy (SEM). The composition profile of these fibers were analyzed by Auger electron spectroscopy (AES). ²⁹Si solid -state NMR spectra of the samples were obtained on a Bruker AV 300MHz spectrometer. XPS was measured by FRR type photoelectron spectrometer at room temperature vacuum and monochromatic Al K α ray. Advanced XRD ray diffractometer and CuK α ray were used as light source to determine XRD data.

3. Results and discussion

Table 1 list the composition and properties of fibers appeared in this paper. According to the Table1 that the resistivity of KD-S and KD-OS is similar, but the resistivity of KD-OSA is two orders of magnitude higher than that of KD-SA. According to its element composition, it is found that there is not much change in the composition of KD-SA after oxidation at 800°C. But we know that free carbon began to oxidize from 400°C, and the carbon-rich layer has great influence on the resistivity of the SiC fibers. So the initial judgment, the sudden rise of the electrical resistivity may cause by the oxidation of the carbon-rich layer.

Table 1. Characterization of the SiC fibers

Sample	Reactive Atmosphere	Temperature (°C)	Chemical composition wt. %			C/Si	Electrical resistivity($\Omega \cdot \text{cm}$)	Tensile strength(Gpa)
			Si	C	O			
KD-S	None	None	65.5	30.3	1.6	1.08	7.0	3.0
KD-OS	O ₂	800	61.2	27.8	1.9	1.06	8.8	2.9
KD-SA	None	None	65.1	30.4	0.8	1.09	30.2	2.3
KD-OSA	O ₂	800	66.2	30.6	1.1	1.08	2961.7	2.0

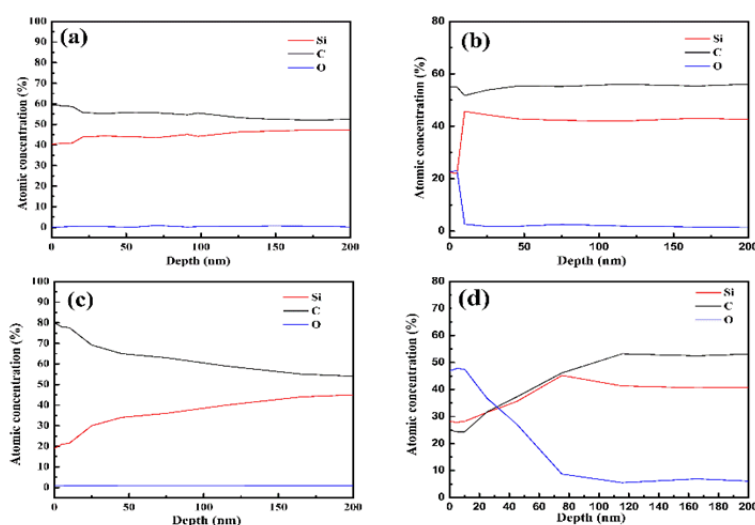


Fig 1. AES composition profiles of the SiC fibers: (a) KD-S; (b) KD-OS; (c) KD-SA; (d) KD-OSA

In order to analyze the radial distribution of fiber composition, AES depth analysis was carried out. As indicated in Fig1, the surface element distribution of KD-S, KD-OS and KD-SA is mainly divided into three parts. The outer layer has a carbon-rich layer at a thickness of about 25nm. In this layer, the concentration of carbon atoms is higher than 50at%. The content of silicon and oxygen in the transition layer increases and the content of carbon decreases gradually between 20 nm and 30 nm. When the dissecting depth reaches 30nm, the fiber composition tends to be stable and the C/Si ratio is about 1.1, which is close to the data of elemental analysis in Table 1. Compared to KD-SA, the thickness of carbon-rich layer on the surface of KD-OSA is decreased and the oxygen content increased obviously, indicating that the carbon-rich layer was oxidized.

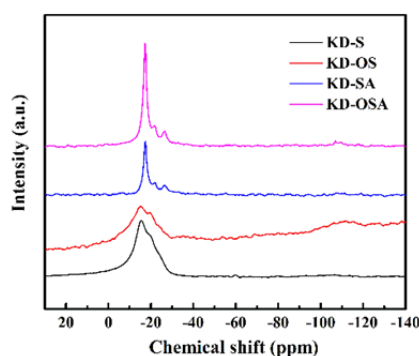


Fig 2. ^{29}Si NMR spectra of the fibers

We measure the AES depth profile of KD-S and KD-SA fiber (Fig.3). Both of them have the carbon-rich layer, but the resistivity of the KD-S fiber is much less than KD-OSA. This indicates that there are other factors which influence the electrical resistivity. According to previous studies^[12,13], the free carbon phase, which is self-assembled within the fibers during pyrolysis, plays an important role in determining the electrical conductivity of the fibers owing to the percolation effect. The electrical resistivity of the fibers is decreased with an increase in the carbon content. The total carbon content and C/Si shown in Table 1 can't really represent the free carbon content in the fiber. The main reason is that the carbon has many forms of binding. Fig 2 shows the ^{29}Si NMR spectra of the fibers. It can be seen from Fig 2 that the resonance peak centered around 0 ppm ($\delta=0$) could be assigned to the resonance of the silicon bonded to four carbons (SiC_4). Signals observed at $\delta = -30, -72$ and -107 ppm could be assigned to the resonances of SiC_2O_2 , SiCO_3 and SiO_4 respectively.^[14] The relative contents of each structure in the four fibers can be calculated by integrating the peaks, as shown in Table.2.

Table 2. Free carbon content data of the SiC fibers

δ		-15	-30	-72		Formula ^a	Formula ^b	ΔC_f	Free carbon content /at%
-107		SiC ₄	SiC ₂ O ₂	SiCO ₃	SiO ₄				
Peak area	KD-S	86.2	13.8	/	/	SiC _{1.08} O _{0.04}	SiC _{0.94} O _{0.11}	0.14	6.6
	KD-OS	82.9	10.0	/	7.1	SiC _{1.06} O _{0.05}	SiC _{0.91} O _{0.18}	0.15	7.1
	KD-SA	90.0	8.9	/	1.1	SiC _{1.09} O _{0.02}	SiC _{0.95} O _{0.08}	0.14	6.6
	KD-OSA	87.7	10.3	/	2.0	SiC _{1.08} O _{0.03}	SiC _{0.94} O _{0.11}	0.14	6.6

SiC_xO_y phase(x+y=4) is the tetrahedron structure of x atom of carbon and y atom of oxygen around silicon. Because carbon can bond with four silicon at the same time, but oxygen atom can only bond with two silicon, the corresponding chemical composition of SiC_xO_y structure should be SiC_{x/4}O_{y/2}. The corresponding chemical composition of SiC₄, SiC₂O₂, SiCO₃ and SiO₄ structures should be SiC, SiC_{1/2}O, SiC_{1/4}O_{3/2} and SiO₂ respectively. The free carbon content can be estimated according to the difference between the element composition of element analysis and the result of ²⁹Si NMR spectra. The computational process and results of the fibers are shown in Table.2. As can be seen from Table.2, both of the free carbon content of KD-S and KD-SA is 6.6%, indicating that the free carbon content is not the reason for the difference in the resistivity of KD-S and KD-OSA fibers.

Besides the free carbon content and the influence of carbon-rich layer, the crystallite size of SiC could also influence the resistivity of the fibers^[15]. The resistivity of the pure material of β -SiC is 7m Ω ·cm^[16] which belongs to the low resistance phase. So with the precipitation of the low resistivity phase β -SiC and the increase of the grain size, the resistivity of the fibers tends to decrease^[17]. The XRD spectra of two kinds of fiber resistivity are shown in Fig.3. From Fig.3, the typical diffraction peaks at $2\theta=35.6^\circ$, 60° and 72° , attributed to the (111), (220) and (311) lattices of β -SiC according to the JCPDS card (29-1129)^[26]. We can see that the peaks of KD-SA are higher and sharper than that of KD-S. As shown in Table 3, the average SiC crystal size is calculated from the half-value width of (111) peak using the Scherrer's formula. It can be seen that the crystal size of KD-SA and KD-OSA fiber is obviously higher than that of KD-S and KD-OS. In accordance with the above rules, the resistivity of KD-S fiber should be higher than KD-SA, but that is not the case, indicating that the difference between the resistivity of KD-SA and KD-S fiber is not caused by the different grain size.

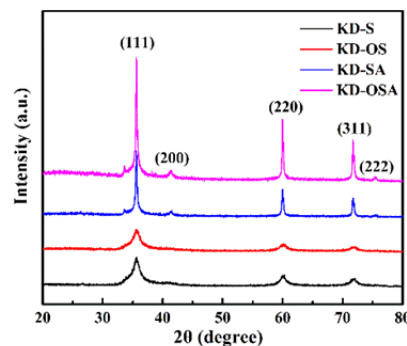
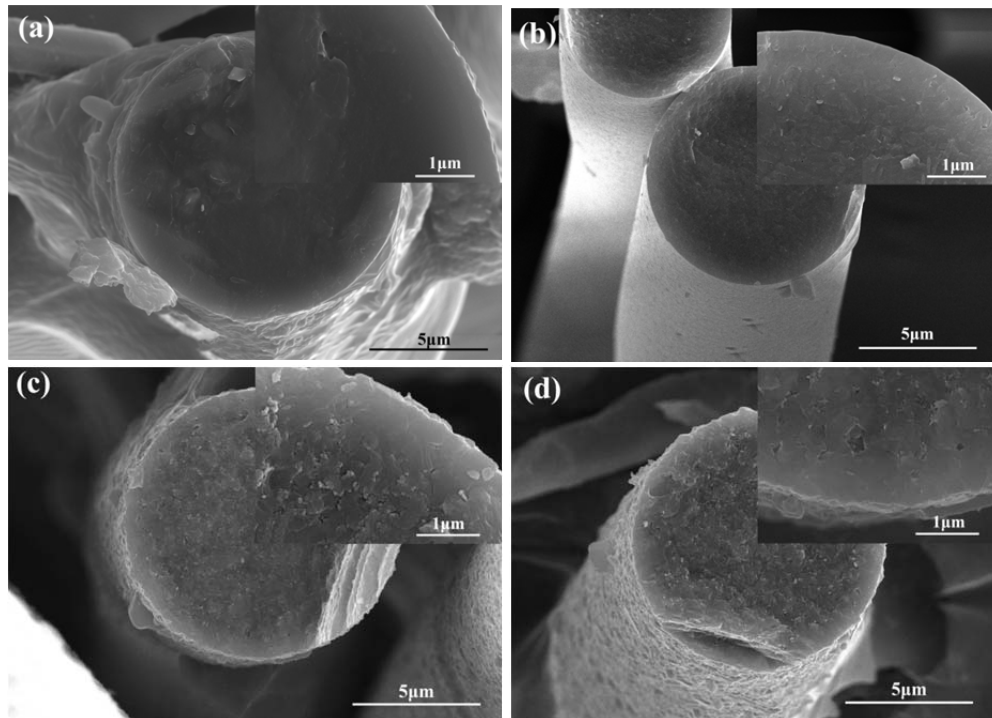
**Fig 3.** XRD curves of the fibers

Table 3. The Crystallite size and Crystallinity of the fibers

Crystalline structure	KD-S	KD-OS	KD-SA	KD-OSA
Crystallite size (nm)	6.0	6.3	55.8	59.6

We know that when the grain grows, the defects in the grains are also increasing, which makes the strength of the fibers decrease, so the strength of KD-SA is slightly lower than that of KD-S fibers. The increase in pore structure fiber affects the conduction of electrons, and the resistivity of the fiber is naturally affected.

The morphologies of the cross section structure of these fibers are shown by SEM micrographs in Fig 4. Fig 4 is the SEM micrographs of the 20000 and 100000 times magnification of the fibers. It can be seen that the cross section of the KD-S and KD-OS belongs to the glassy cross section without any obvious pores and defects. However, coarsened β -SiC grains and the pores were found in the cross section of KD-SA and KD-OSA fibers which proves the conjecture above.

**Fig 4.** Cross section of the SiC fibers: (a) KD-S; (b) KD-OS; (c) KD-SA; (d) KD-OSA

As the density of C and Si is 2.26, 2.33 g/cm³, respectively, lower than the density of SiC(3.21 g/cm³)^[18]. Therefore, the density of stoichiometric SiC fiber is the largest, but both KD-S and KD-SA are near stoichiometric fibers. So the difference of the density of the fiber may cause by the pore structure in the fibers. Formula (1) can calculate theoretical density (ρ_t) of different fibers, in which the ρ_i means the density of the constituent, V_i means the volume fraction of the constituent, and thus can calculate fiber porosity by formula (2):

$$\rho_t = \sum \rho_i V_i \quad (1)$$

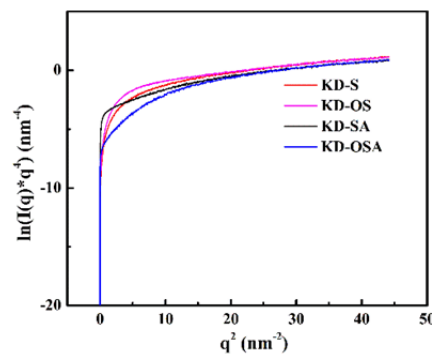
$$P = 1 - (\rho / \rho_t) \quad (2)$$

As shown in Table 4, it can be seen that the porosity of KD-SA and KD-OSA fibers is higher than that of KD-S and KD-OS fibers. Comparing the resistivity of KD-SA and KD-S fibers, it is found that the larger the pore size, the higher the resistivity.

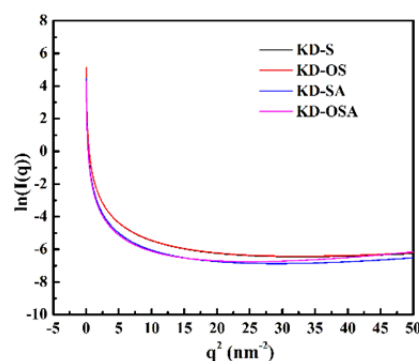
Table 4. Density and porosity of SiC fibers

Fiber	C/Si	Mole composition	Actual density (g/cm ³)	Calculated density (g/cm ³)	Pore fraction(%)
KD-S	1.08	SiC+0.08C	2.91	3.18	8.4
KD-OS	1.06	SiC+0.06C	2.89	3.19	9.2
KD-SA	1.09	SiC+0.09C	2.70	3.17	15.0
KD-OSA	1.08	SiC+0.08C	2.72	3.18	14.4

Small angle X-ray scattering (SAXS) is a useful tool for the study of the structure of porous materials with nano-sized pores. The principle is that the X-ray scattering is caused by the difference in electron density between the material matrix and the micropore. It can not only study the open pore can also study the blind pore. The fiber's X-ray scattering come from the pore, and may also come from the β -SiC grains and carbon particles. Lipowitz calculate the scattering energy to confirm that the SAXS scattering of SiC fiber is mainly caused by the pore, rather than β -SiC grains and carbon particles^[19,20].

**Fig.5** Porod plots of the fibers

The scattering by an ideal two-phase porous system with sharp boundary obeys Porod's law. After deducting the background of SAXS data, the Porod curve, is shown in Figure 5. The Porod curves of KD-S and KD-OSA fibers are positive deviations, indicating that there are still small size microstructures below 1nm in the fiber except for the scattering by the micropore^[21].

**Fig.6** Guinier curves of the fibers after Porod correction

If there are disorder or thermal density fluctuation within solid phase, it will give rise to an additional relatively low scattering mixed with the SAXS intensities of pores and then lead to a positive deviation from Porod's law. It is therefore necessary to correct the deviation for studying the pore structure, and then the Guinier curve can be obtained by using the Porod corrected curve data, as shown in figure 6. The Guinier curves of the fibers showed a concave tendency, indicating that the scattering system was a multi-dispersed system, and the distribution of the micropore size in the fiber was observed^[22].

In order to deduce the micropore size distribution of polydisperse system, we adopt the tangent method proposed by Jellinek and Frankuchen in 1946. Using this method, the micropores are divided into several levels, and this method can be used to calculate the micropore content of different gyration radius (R_g)^[23]. The mean radius of rotation is derived. The gyration radius of rotation is the root-mean-square distance between all electrons of the scatterer and the center of gravity of the electron, and can be used as a statistical scale to indicate the size of the scatterer, which is suitable for the scattering body of any shape. Therefore, it is an important parameter in SAXS. For the convenience of study, the shape of the micropore in the fiber can be simplified into a spherical micropore, and its radius r_s and diameter d_s are changed from $R_g=(3/5)^{0.5}r_s$ ^[24] and $d_s=2r_s$, the pore size distribution of the fibers is obtained, and the average micropore size is calculated as shown in Table 5. We can see that the average pore size of micropore size of KD-SA was higher than KD-S, and the resistivity of KD-SA was increased, which proves the effect of pore structure on the resistivity of fiber.

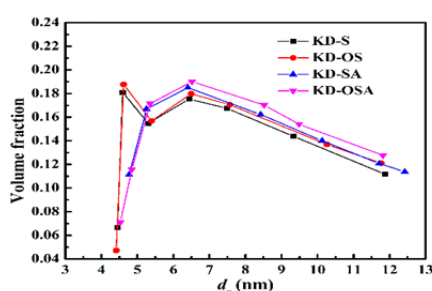


Fig.7 Size distribution of micropores in the fibers

Table.5 Mean size of micropores in the fibers

Fiber	Mean R_g (nm)	Mean d_s (nm)
KD-S	2.7	6.9
KD-OS	2.8	7.2
KD-SA	3.2	8.2
KD-OSA	2.9	7.5

4. Conclusion

First, we find that all of the KD-S, KD-OS and KD-SA fibers have the carbon-layer through the AES analysis, and the resistivity of KD-OS is similar with that of KD-S, lower than KD-SA. But after oxidation at 800°C, the carbon-rich layer on the surface of KD-SA fiber damaged and get the KD-OSA fiber. Meanwhile, the resistivity of the fiber goes from $10^1 \Omega \cdot \text{cm}$ to $10^3 \Omega \cdot \text{cm}$. Then, Comparing the structure of four fibers through ^{29}Si NMR analysis, we find that they have the similar free carbon content. Moreover, we compared the crystalline structure of four fibers and observe that the grain size of KD-SA and KD-OSA is much larger than that of KD-S and KD-SA, which can't explain the different resistivity between KD-SA and KD-S. So there are other factors which affect the fiber resistivity. We compared the pore structure between KD-S and KD-SA fibers by SEM, bulk density measurements and SAXS, so that when the pore structure of the fiber is rich, the pore size is larger, easier to hinder the conduction electrons in the fiber, which makes the resistivity rise.

References

- [1] Laine R M , Babonneau F. Preceramic polymer routes to silicon carbide. Chem Mater, 1993,5:260—279.
- [2] Birot M, Pillot J P, Dunogues J. Comprehensive chemistry of polycarbosilane, polysilazane, and polycarbosilazane as precursors of ceramic. Chem Rev,1995,95(5):1443—1477.
- [3] Mazdiyasn K S. Fiber Reinforced Composites :Materials ,Processing and Technology. Park Ridge, NJ :Noyes Publication,1990:199 -243.
- [4] Yajima S,Hasegawa X,Hayashi J, et al. Synthesis of continuous SiC fibers with high tensile strength and modulus. J Mater Sci,1978,13:2569—2576.
- [5] Yajima S , Hayshi J,Omori M,et al. Development of a SiC fibre with high tensile strength .Nature,1976,261:683—685.
- [6] S.Y.Cao, J.Wang, H.Wang, et al. Influence of free carbon elimination on microstructure and property of SiC fibers. J Inorgan Mater, 2016, 31(5): 529-534.
- [7] D.Y.Wang, X.H.Mao, Y.C.Song, et al. Preparation and properties of SiCfiber with a stable excess

- carbon layer on the surface. *J Inorgan Mater*, 2009, 24(6): 1209-1213.
- [8] D.Y.Wang. Preparation and characterization of continuous silicon carbide and silicon oxynitride fibers. Master Dissertation. Changsha: National University of Defense Technology, 2011.
- [9] T.J.Hu, X.D.Li, G.Y.Li, et al. Models proposed to explain the electrical conductivity of polymer-derived silicon carbide fibers. *J Am Ceram Soc*, 2017, 100: 167-175.
- [10] Y.Z.Gou, H.Wang, K.Jian. Facile synthesis of melt-spinnable polyaluminocarbosilane using low-softening-point polycarbosilane for Si-C-Al-O fibers. *J Mater Sci*, 2016, 51: 8240-8249.
- [11] Z.F.Xie, Y.Z.Gou. Polyaluminocarbosilane as precursor for aluminum containing SiC fiber from oxygen-free sources. *Ceram Int*, 2016, 42: 10439-10443.
- [12] G.Chollon, R.Pailler, R.Canet, et al. Correlation between microstructure and electrical properties of SiC-based fibers derived from organosilicon precursors. *J Eur Ceram Soc*, 1998, 18(6): 725-733.
- [13] D.Y.Wang, Y.C.Song, K.Jian. Effect of Composition and Structure on the Specific Resistivity of Continuous Silicon Carbide Fibers. *J Inorgan Mater*, 2012, 27(2): 162-168.
- [14] X.D.Li, M.J.Edirisinghe. Evolution of the ceramic structure during thermal degradation of a Si-Al-C-O precursor. *Chem Mater*, 2004, 16(6): 1111-1119.
- [15] M.Narisawa, Y.Itoi, K.Okamura. Electrical resistivity of Si-Ti-C-O fibers after rapid heat treatment. *J Mater Sci*, 1995, 30(13): 3401-3406.
- [16] K.Luo, N.L.Shi, Y.D.Duan. Impedance Characteristics and Specific Resistance of Electrochemically Treated CVD SiC Fibers. *Aer Mater Tech*, 2001(3): 45-48.
- [17] T.Shimoo, Y.Katase, K.Okamura, et al. Carbon elimination by heat-treatment in hydrogen and its effect on thermal stability of polycarbosilane-derived silicon carbide fibers. *J Mater Sci*, 2004, 39(20): 6243-6251.
- [18] M. Takeda, A.Saeki, J.I.Sakamoto, et al. Effect of hydrogen atmosphere on pyrolysis of cured polycarbosilane fibers. *J Am Ceram Soc*, 2000, 83(5): 1063-1069.
- [19] J.Lipowitz, J.A.Rabe, L.K.Frevel, et al. Characterization of nanoporosity in polymer-derived ceramic fibers by X-ray scattering techniques. *J Mater Sci*, 1990, 25: 2118-2124.
- [20] J.Lipowitz, H.A.Freeman, R.T.Chen, et al. Composition and structure of ceramic fibers prepared from polymer precursors. *Adv Ceram Mater*, 1987, 2: 121.
- [21] M.Zhang, F.L.Meng, Z.F.Meng. A study on the Micro-fluctuation of density in graphite matrix of the carbon fibre by SAXS. *ACTA Sci Nat Univ Jilin*, 1997, 1(1): 66-68.
- [22] D.H.Li, G.P.Wu, C.X.Wu. Pore size distribution of microspore in PAN-based carbon fibers and their precursors. *J Instrumental Anal*, 2010, 29(4): 321-326.
- [23] Z.F.Meng, Theory and application of SAXS. Chang chun: 1996, 28-35.
- [24] W.Wang, X.Chen, Q. Cai, et al. In situ SAXS study on size changes of platinum nanoparticles with temperature. *Eur Phys J B*, 2008, 65: 57-64.
- [25] Guinier A, Fournet G, C.B.Walker. Small-angle scattering of X-rays. New York: John Wiley & Sons, Inc, 1955.
- [26] H.Wang, B.Gao, X.Chen, et al. Synthesis and pyrolysis of a novel preceramic polymer PZMS from PMS to fabricate high-temperature-resistant ZrC/SiC ceramic composite, *Appl. Organomet. Chem.* 2013, 27(3):166-173.